SLINGATRON: A HIGH VELOCITY RAPID FIRE SLING

D. A. Tidman

Advanced Launch Corporation, 6801 Benjamin Street, McLean, VA 22101-1576
datidman@starpower.net

The mechanics of a spiral slingatron mass accelerator is discussed, together with some experiments to measure the sliding friction and mass loss of projectiles in such a machine. The potential utility of this machine for defense applications is also discussed, including examples of 1 kg and 50 kg projectiles launched at 3 km/sec. The device appears capable of high launch velocity with repetitive fire without over-heating the steel guide tube, since hot high-pressure gas is not used. It could derive power from a turbine that burns kerosene and it fires projectiles without propellant cartridges. Angular dispersion of emerging projectiles can be minimized, but would be larger than for conventional guns. However, projectiles that are smart enough to reduce dispersion of the projectile stream would suffice for many applications. Smart projectiles would also be needed for any gun capable of the long-range missions available due to high launch speed.

INTRODUCTION

A mechanical mass accelerator concept called a slingatron has been proposed by the author [1-5] and computer models developed by Tidman [2], Cooper et al [6], and Bundy et al [7] for the dynamics of both spiral and circular versions of this machine. Here we first summarize the dynamics. A new approach to the mechanics is then discussed that is useful for the potential defense applications of a spiral slingatron in which a projectile (or stream of projectiles) could be accelerated to high velocity.

The device consists of a spiral steel tube (Fig.1) mounted on swing arms distributed along it so that the entire tube can be propelled so that it gyrates around a small circle of radius r with a *constant* gyration frequency f cps. The machine transfers stored inertial energy directly into projectile kinetic energy with no intermediate steps, and work is done on a projectile sliding through the spiral because the accelerator tube is continually pulled inward at the projectile location against the centrifugal force of the projectile. The accelerating force experienced by the projectile is an example of a coriolis force and is proportional to the projectile mass. As the projectile swings out around the spiral into turns of increasing radius R, it also maintains phase stability with the small-radius gyration of the entire tube. This phase locking enables it to move out around the spiral turns with the same frequency f so that its increasing velocity V is approximately equal to $2\pi Rf$. The device can be viewed as a mass cyclotron [2].

The dynamics is similar (but not identical) to whirling a mass around at the end of a string as in a conventional sling, but with the string growing in length so that the whirling frequency, f cps, is constant. However, there is a basic difference in that there is no string to break under tensile stress in the slingatron. Instead, the guide tube can contain

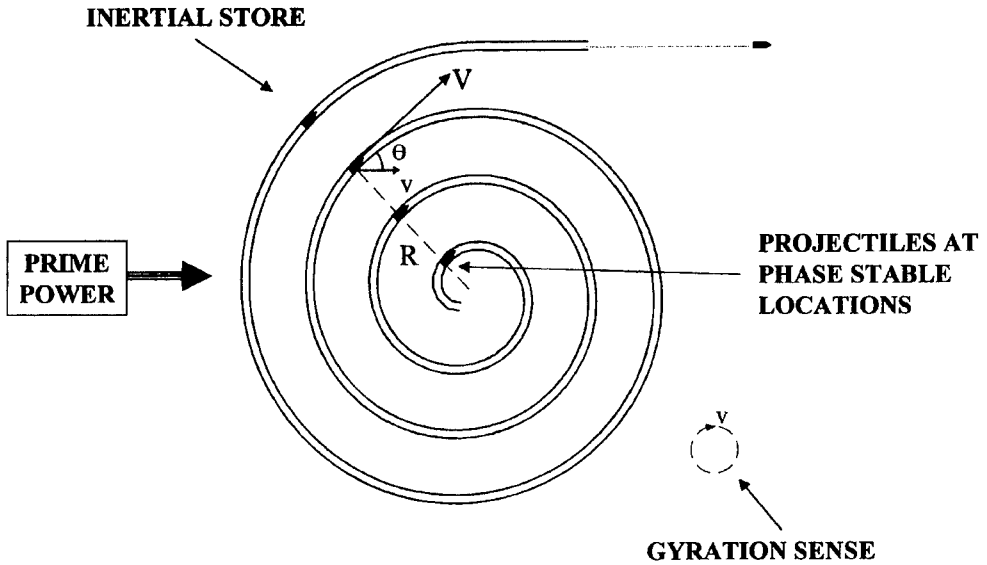

FIGURE 1. A Spiral Tube mounted on Distributed Swing Arms (not shown) that propel the entire spiral around a Small Gyration Circle of radius r with a Constant Frequency f cps and the sense shown. Projectiles fed into the Spiral Entrance are pushed forward by the Closed Breech and accelerate through with a Stable Relative Phase Angle θ and Increasing Speed $V = 2\pi Rf$.

the projectile to much higher speeds since the mechanical impulse delivered per unit length, $mV/R \cong 2\pi mf$, is approximately constant along the spiral. The tube wall thickness can thus remain constant along the spiral.

Note that if one treats the tube as an elastic beam supported at intervals on swing arms, the driving force per unit length in the beam deflection equation swept by a point mass m would be $(mV^2/R)\delta(x - Vt) = \hat{\pi}mf\delta(t - x/V) \rightarrow \hat{\pi}mf\delta(t)$ as $V \rightarrow \infty$, i.e., a uniform impulse for segments traversed with V >> transverse wave speeds. The projectile wave drag due to the elastic response of the track is also small for all speeds.

Experimentally, we have repeatedly fired 0.738 gram lexan projectiles at 5.2 km/sec into curved 1020 steel tube (OD = 0.5, ID = 0.3, wall thickness of 0.1in.) and a radius of curvature R = 30 inches, so that a force of 2.7 tons sweeps around the tube with a contact bearing pressure of 1.37 kbars, and with no discernable effect (except to slightly smooth the tube asperities). A static force of this magnitude would permanently deform the tube.

For most defense slingatrons a single conventional motor could be used to propel the gyration, and for larger systems distributed motors could be used to swing the spiral around its gyration circle and continuously supply inertial energy globally to the spiral for extraction by an ongoing stream of projectiles passing through the spiral. The launcher could be operated as a rapid-fire device with a maximum shot frequency equal to the gyration frequency f (assuming the prime power is available), and for a given design its system mass is approximately proportional to mV^2, [5].

No gun injector is needed. A projectile inserted into the spiral entrance with the breech closed behind it will accelerate through the spiral. It will acquire its initial speed when the tube is moving forward at the projectile location, so that the projectile initial speed (acquired from the breech block) is the same as the gyration speed $v = 2\pi rf$. In this case it is also necessary for the first turn of the spiral to have a radius of curvature that is no more than a few times the gyration radius, and an interior diameter slightly larger than the projectile diameter so that the projectile can negotiate the first turn. A mechanical feed of projectiles into the entrance can then maintain the supply of projectiles.

Note also that the absence of hot propellant gas in the guide tube allows a higher velocity, projectile mass, and fire rate, than conventional guns without overheating the guide tube. A slingatron also has no appreciable muzzle blast or EMP, other than what might arise from the drive motor. Although the spiral guide tube is long, it could be constructed from segments with tapered entrances at the connections. The machine is not sensitive to the exact shape of the spiral, which could approximate an Archimedes spiral.

The two basic issues involved in construction of a slingatron are the sliding friction coefficient of the projectile (with its attendant mass loss), and implementation of the mechanical system needed to propel the gyration.

APPROXIMATE RELATIONSHIPS FOR THE DYNAMICS

The approximate equations listed here are useful for guideline purposes as a supplement to the computer models based on more exact equations. An approximate equation of motion for the projectile in a spiral sling can be obtained, Fig.1, by equating the rate of energy gain for the projectile, $(d/dt)(0.5mV^2)$, to the power used to pull against the projectile centrifugal force $(mV^2/R)v\sin\theta$, minus the power dissipated by the projectile sliding friction, $\mu mV^3/R$. Note, all three of these powers neglect higher order terms in the small quantities r, v, and μ, and for this discussion we also assume that the projectile mass m is constant. The result is

$$dV/dt \cong (V^2/R)(vV^{-1}\sin\theta - \mu), \qquad (1)$$

where R is the guide tube radius of curvature at the projectile location, V the projectile speed in the spiral tube, v the constant gyration speed (assumed << V), and θ is the phase angle between the vectors **v** and **V**. It is also assumed that projectile drag due to residual gas in the guide tube is negligible, so that μ is simply the sliding friction coefficient. We also consider only spirals for which the gap between neighboring turns is a constant.

We see from equation 1 that the key to achieving a high projectile velocity is to mechanically implement a high gyration speed v, and for the projectile to have a small coefficient of sliding friction and to lose only a moderate amount of its mass to supply the gas film on which it slides.

When the exact equations for the dynamics are solved numerically, one finds that for most of the range $0 < \theta < \pi/2$, the projectile is stably trapped in a traveling potential well and advances around the spiral turns with an angular frequency V/R approximately equal to $v/r = 2\pi f$, i.e., acceleration occurs. Provided the friction term μ remains smaller than $v\sin\theta/V$ (because μ is decreasing with increasing V), the angle θ undergoes only

small oscillations about (and a small cumulative displacement in) its stable value to accommodate changes in the relative magnitudes of the coriolis and friction terms. Phase locking occurs, Fig. 1, because if a perturbation causes the projectile to move too fast its relative phase θ decreases and the gyration velocity component perpendicular to the tube at the projectile location decreases (as does the rate at which work is done against its centrifugal force) and the projectile falls back, and conversely if it moves too slowly its relative phase θ increases so the projectile experiences a larger accelerating force and catches up. Computer models and analysis show that friction damps oscillations about the stable relative phase as the projectile advances through the spiral.

As long as this situation prevails, and acceleration continues, it suffices to assume

$$V/R \cong 2\pi f = v/r. \qquad (2)$$

For a spiral designed with constant gaps ΔR between its turns, the velocity gain per turn, ΔV, is also approximately constant, in which case

$$\Delta V \cong 2\pi(v\sin\theta - \mu V), \qquad \Delta R \cong 2\pi(r\sin\theta - \mu R)\,, \qquad (3)$$

and the relative phase θ changes slightly to accommodate the change in μ. For example, for a gyration speed v = 200 m/sec and $\theta = \pi/3$ with m constant and friction negligible, the gain in velocity per turn would be $\Delta V \cong 1$ km/sec. A more complete list of approximate formulas for the case m = constant has been given earlier [5], and exact equations and computer models for the dynamics in references [2,6,7] with [6] including discussion of projectile mass loss.

Finally note that the guide tube has a radius of curvature R that goes from R_{in} for the inner turn to R_{out} for the outermost turn. If the projectile consisted of a perfectly rigid cylinder of length l_p, it would be supported in the tube on its two ends with its mid-section above the tube surface a height δh given approximately by $\delta h/l_p \cong l_p/8R << 1$. However, δh becomes sufficiently small after passing through the first 1 or 2 turns, and the centrifugal force sufficiently large, that projectile elasticity provides the small amount of flexure (well below its elastic limit) needed to push it into tight contact with the tube along the projectile length. As the projectile travels farther out through the spiral its flexure decreases as R increases, and could be reduced to zero at exit by gradually straightening out a segment of tube and bringing its ID down to fit the projectile diameter just before the exit.

MECHANICAL DESIGN

The slingatron is subjected to two kinds of stress, Harris [8] and Tapley [9], namely quasi-static stresses due to gyration and a traveling impulse due to the projectile. Impulsive stresses can be treated approximately using an energy method, or by using detailed codes. In this section we briefly discuss only the gyration machinery and leave a safety margin so that a range of applicability that includes the traveling impulse of the projectile could be experimentally determined.

In order to swing the entire spiral around its gyration circle of radius r, the guide tube is attached to swing arms via clamps that turn on tapered roller bearings as shown in Fig. 2. These bearings allow the entire spiral to roll around its gyration circle while keeping its orientation the same, i.e., it gyrates but does not spin. The swing arms could be oblique to the gyration plane of the spiral tube, which allows them to be spaced more closely along the tube without mutual collision occurring, which in turn allows a higher swing speed without shear of the guide tube. Close packing of the clamps also avoids resonance between the gyration frequency f and transverse elastic vibrations of the tube segments. For example in Fig. 2 they are shown spaced so that the tube segment length between the centers of adjacent clamps is $L_{seg} = r$. For early experiments however, it might be simpler to swing the arms in a plane with $L_{seg} \cong 1.5r$.

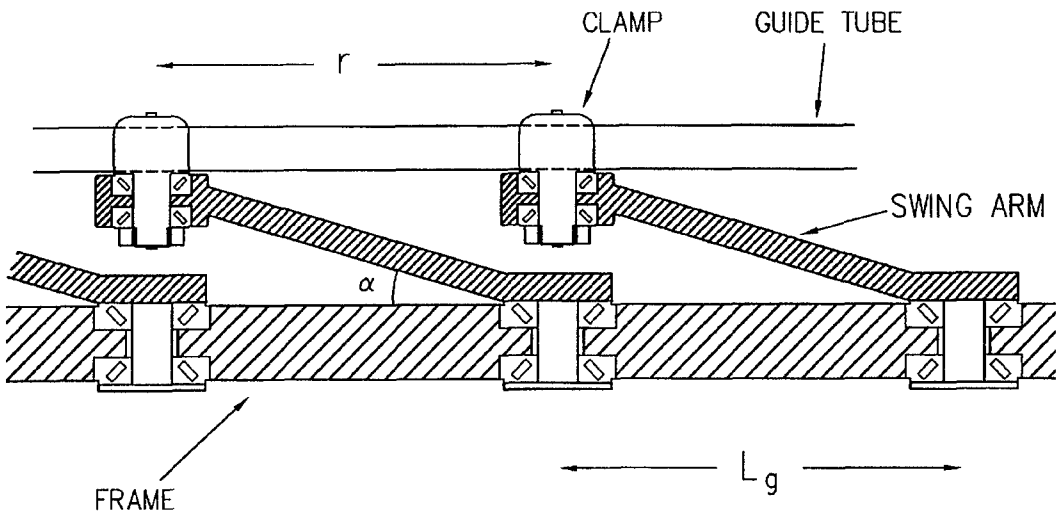

FIGURE 2. Distributed Swing Arms are shown Oblique to the Spiral Plane for Close Packing along the Guide Tube for Maximum Swing Speed. Arms could alternatively be deployed both above and below the guide tube. The arms have a cross-sectional area A that is larger at the frame (they are wider plates going into the page) and A decreases along the arm toward the end that clamps to the tube.

Swing Arms and the Potential for High Gyration and Projectile Speeds

We consider the case in which the arms in Fig. 2 swing in a plane, i.e., $\alpha = 0$, which can also be viewed as an approximation for long swing arms with a small finite value for α. The arms then experience tensile stress that remains approximately parallel to a swing arm as it swings around the gyration circle. If we choose to use 4340 (Q&T, 315C) steel for the arm, a design strength of T = 120,000 psi can be assumed, which is approximately its fatigue endurance limit for cycled stress (even though this stress is not cycled). This allows some added strength for the traveling impulse delivered by the projectile sweeping around the spiral.

If we design the arm with a cross-sectional area A(r) that decreases going away from the frame so that its tensile stress T is constant in the arm, i.e., there is no parasitic mass being carried in the arm, we find the result $A(r) = A_o\exp(-2\pi^2\rho f^2 r^2/T)$, where ρ is the steel density and A_o the cross-section at the frame. The swing speed is then

$$v = 465[\ln(A_o/A)]^{1/2} \quad \text{meters/sec,} \qquad (4)$$

and the mass m_{load} that can be carried at the end of the arm (consisting of the tube segment, clamp, bearings, and steel to retain the bearings) is given by $m_{load} = AT/(4\pi^2 rf^2)$.

However, the clamps and guide tube experience stresses that are both cycled and in the shear direction, so that more complicated geometrical factors are involved in their stress distributions. For these components we choose a design strength S = 60,000 psi for 4340 steel.

Consider the maximum average shear stress at the clamped ends of a tube segment of length $(L_{seg} - L_{clamp})$ between clamps of length L_{clamp} and density ρ propelled around a circle of radius r with a frequency f cps. This stress is $2\pi^2 f^2 \rho r(L_{seg} - L_{clamp})$ so that the maximum speed with which the tube segment can swing around is,

$$v(max) = (2Sg_E r/\rho(L_{seg} - L_{clamp}))^{0.5} = 320(r/(L_{seg} - L_{clamp}))^{0.5} \quad \text{meters/sec,} \qquad (5)$$

where we used $g_E = 386$ in/sec^2, $\rho = 0.289$ lbs/in^3, and could allow the clamp to be tapered and extend a length L_{clamp} along the tube for tube support so that the tube segment effective length shown in Fig. 2 is reduced.

In summary we see that very high swing speeds are possible. For example for v = 300 m/s the projectile velocity gain per spiral turn follows from (3) as $\Delta V = 1.6$ k/s/turn, neglecting friction and assuming a phase locked angle $\theta = \pi/3$. Conceivably a future machine using advanced materials (in a reduced pressure environment) might achieve a swing speed of v = 1 km/sec, in which case $\Delta V = 5.4$ km/sec/turn, i.e., V = 21 km/sec in four turns! But a first-generation machine is likely to operate in the range $v \sim 200$ m/s.

There will be some binding of the motion due to clamping of the tube at multiple locations, but as the spiral gains speed the centrifugal forces rapidly become dominant as the tube pulls outward against the swing arms, as was found in a small machine [2].

Reciprocating Machinery for Synchronous Drive

Consider first the case of a *single* swing arm with its shaft bearing anchored in a drive plate as shown in Figure 3(a). If the drive plate is propelled in a small radius circular motion, energy can be pumped into the swing arm rotational motion. This swing arm motion can be stably phase-locked with the drive plate motion just as for a conventional sling (in which ones hand replaces the plate) or for a projectile accelerating in a gyrating spiral as discussed earlier.

Thus if a number of such swing arms were anchored in a drive plate as in Figure 3(b), they could *all* be synchronously accelerated (once started) by a small-amplitude circular motion of the drive plate, regardless of possibly differing masses and swing arm lengths. This phase stability allows a complete spiral guide tube, clamped by distributed swing arms as in Figure 3(c), to be accelerated up to a high gyration speed while maintaining

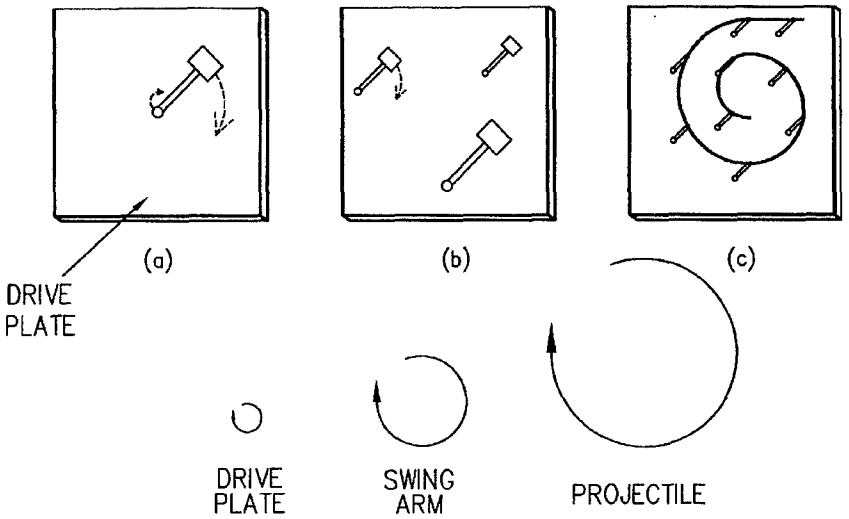

FIGURE 3. Phase Stability maintains Synchronization of the Swing Arms propelled by a Small-Amplitude Circular Motion of a Drive Plate. The Plate Motion is the same as one makes by hand in whirling a Conventional Sling.

synchronization along the guide tube length. No other provision for synchronization between the arms is needed. Guide tube stiffness suffices to start the motion of the spiral in a synchronized state, and phase locking maintains it thereafter.

Another way to view this is to regard Figure 3(a) as simply an example of a small mass orbiting about a larger mass, and tied together by a swing arm. Assume for the moment that the system is not being driven and that the drive plate is confined to slide in a plane with frictionless bearings at its four corners. These two masses then cycle around each other in a plane, and the end of the swing arm moves around a circle of radius r and the heavier plate moves around a smaller circle of radius δr. Note that these *radii* are *independent* of the gyration speed. Also, although the centrifugal forces can become large, they are balanced and distributed internally in the coupled system, just as for a top spinning about its center of mass.

Figures 4 and 5 show an example utilizing this drive principle in which a single automobile engine is used to power the small-amplitude drive plate motion. The drive plate is captured at its four corners by bearings that constrain its motion to a horizontal plane. This restraint involves a relatively small oscillating vertical force (moment) due to

the fact that the drive plate and the guide tube cycle in planes that are slightly displaced from each other. Two camshafts propel the circular motion of the drive plate but do not experience the large internal centrifugal forces provided they push the drive plate around a circle of radius equal to the natural cycling radius of the drive plate.

The system is essentially a two-stage sling. The cams at the ends of the two vertical shafts in Fig 5 propel the drive plate around a small circle, and the drive plate in turn slings the spiral around a larger circle, and the spiral slings the projectile around and even larger radius path with very high speed. All three of these motions occur at the same frequency but with ascending velocities, and the sling motions are phase stable. Also, little energy would be stored in the drive plate motion.

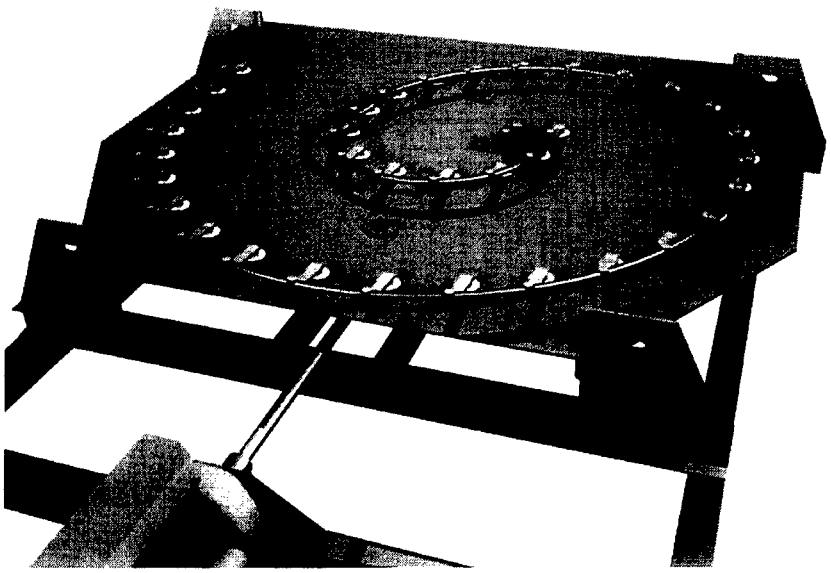

FIGURE 4. Concept for a 1.5-Turn Spiral Experiment Powered by an Automobile Engine. Two Vertical Camshafts under the plate power the plate motion and are shown in Figure 7. A small Clip of Cartridges is shown for supplying a Short Burst of Projectiles. The Drive Plate could have holes to make it lighter.

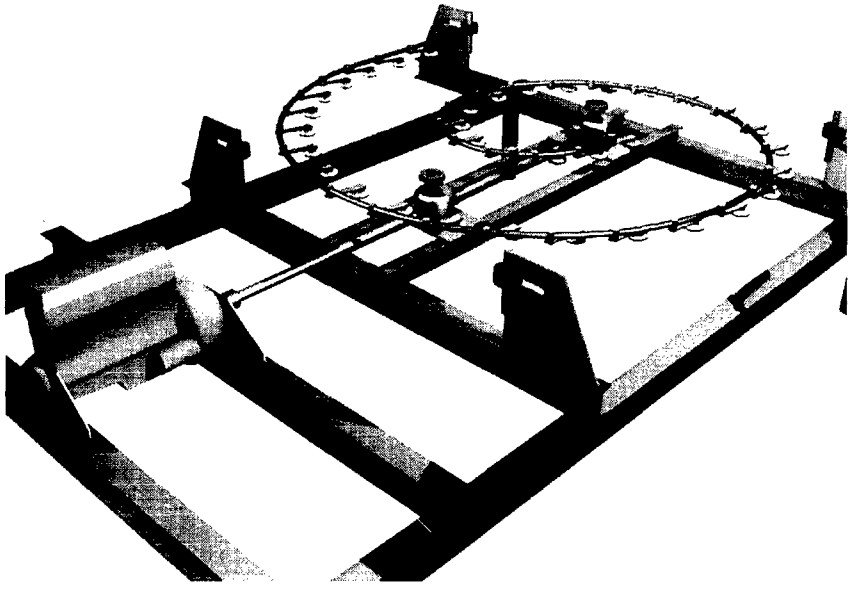

FIGURE 5. The same system as Figure 6 but with the Drive Plate removed to show the Motor Shaft passing through two Gear Boxes with their Vertical Camshafts that propel the Drive Plate.

Role of Air Drag

The gyrating components consisting of the swing-arms, guide tube, clamps, etc, experience aerodynamic drag as they swing around the gyration circle at speed v. In addition, the projectile will snowplow air (and in rapid fire cases also bearing gas) in the guide tube, but this could be vented through slots on the inner side of the curved tube as shown in the table top machine in Fig. 4 of Ref. 2.

For a rapid-fire system the power inputs required to drive the system typically have relative magnitudes (Power to Maintain Projectile KE Stream) > (Aerodynamic Swing-Drag Power) > (Roller Bearing Friction Power of Drive Modules). This assumes a drag coefficient $C_D \sim 1$ for the arms, clamps, and guide tube, and also assumes that the fire rate is > 0.1f. Although one could reduce the swing drag by streamlining the design of the gyrating components to reduce C_D, this might not be worth doing for the case of a rapid-fire system since the prime power input required is in any case dominated by the kinetic energy power of the projectile stream.

For spirals designed for extremely high projectile velocity (e.g., physics experiments) one could eliminate air drag by enclosing the entire system in a reduced-pressure environment. These involve long tapered swing arms with high swing speeds v.

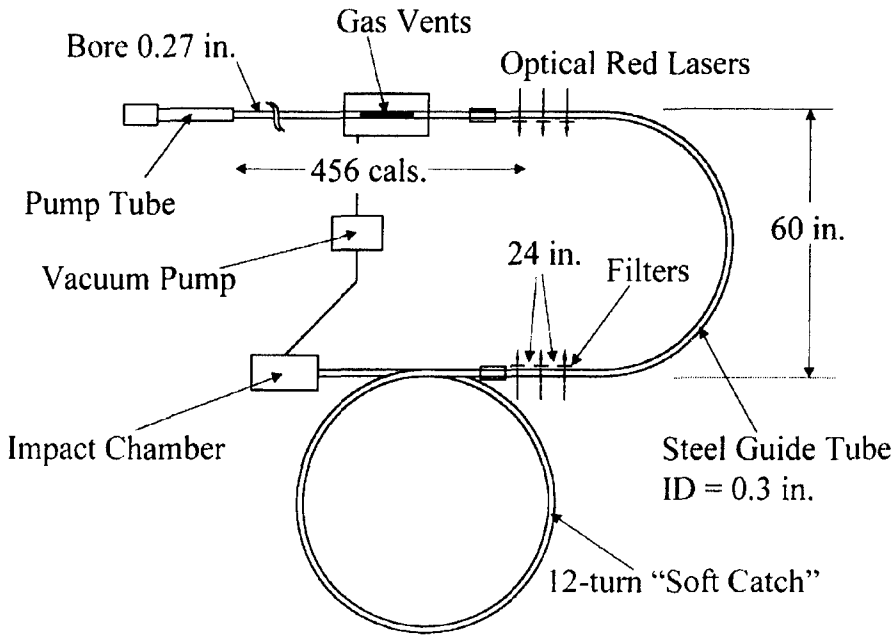

Figure 6. Layout of the Sliding Friction and Mass Loss Experiment.

SLIDING FRICTION AND MASS LOSS EXPERIMENTS

Here we give a brief summary of experiments described more fully in Ref 10. Figure 6 shows the layout of the experiment used to obtain data for the projectile velocity loss and mass loss due to friction up to ~ 4 km/sec. It consists of a 2-stage light gas gun of small bore size, namely 0.27 inches, that fired lexan projectiles of mass 0.738 grams into evacuated semicircular guide tubes of various radii, after which the projectile came to rest in a 12-turn ring that functioned as a soft catch .

The laser triplets located at the input and output ends of the semicircular guide tube provided a measurement of the projectile velocity V_{in} going into the curve, and V_{out} leaving the curve. As the projectile passes through the semicircle it is pushed against the outer wall of the tube which results in a frictional force $-\mu mV^2/R$. In Fig.7 we plot data for the quantity $\pi^{-1}\ln(V_{in}/V_{out})$, as a function of the average velocity $V = 0.5(V_{in} + V_{out})$ around the semicircle, and in all cases the velocity loss $V_{in} - V_{out}$ was small compared with V_{in}. The relationship of $\pi^{-1}\ln(V_{in}/V_{out})$ to μ follows from equation 1 (with $v = 0$) but generalized to include a drag term due to bearing gas accumulated on the projectile nose, and also to allow for projectile mass loss. Converting the time derivative d/dt to Vd/dx, and integrating along the projectile path around the semi-circle then gives,

$$\pi^{-1}\ln(V_{in}/V_{out}) = \mu - (2\pi)^{-1}\ln(m_{in}/m_{out}) + 0.25\pi d^2 R\langle P_{nose}/(mV^2)\rangle \ , \qquad (6)$$

where the subscripts in and out indicate the projectile velocity or mass either entering or leaving the semicircular tube section, d is the projectile diameter, R the radius of the semicircular tube, P_{nose} the reverse pressure from the dusty gas mass that accumulates on

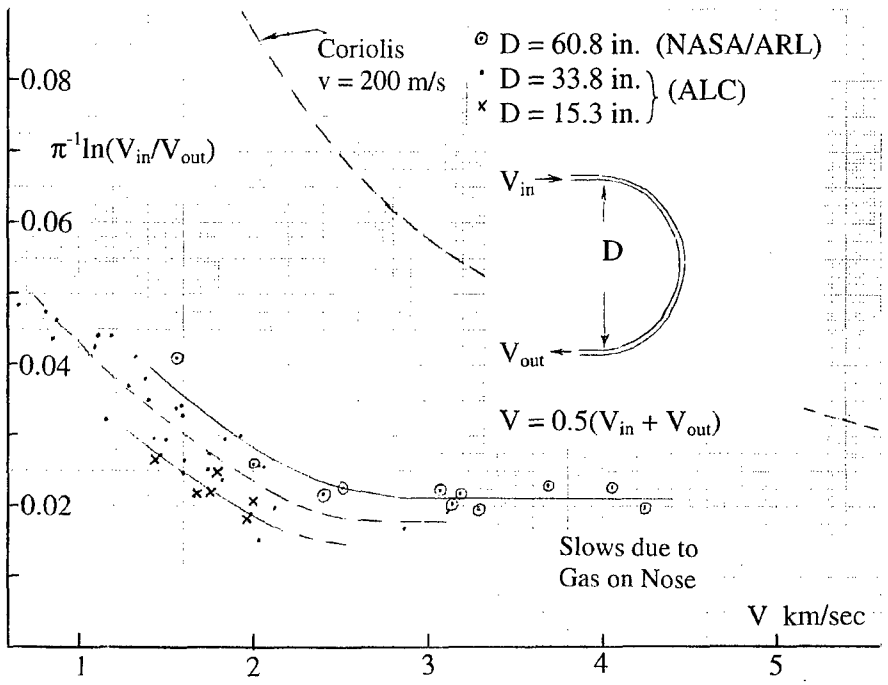

FIGURE 7. Velocity Slowing Data for 0.738 gram lexan Projectiles fired through a Semicircular Arc of Steel Tube for several values of the Arc Diameter D = 2R and Injected Velocities V_{in}. The Relationship of the Quantity Plotted to the Friction Coefficient is given by equation 6.

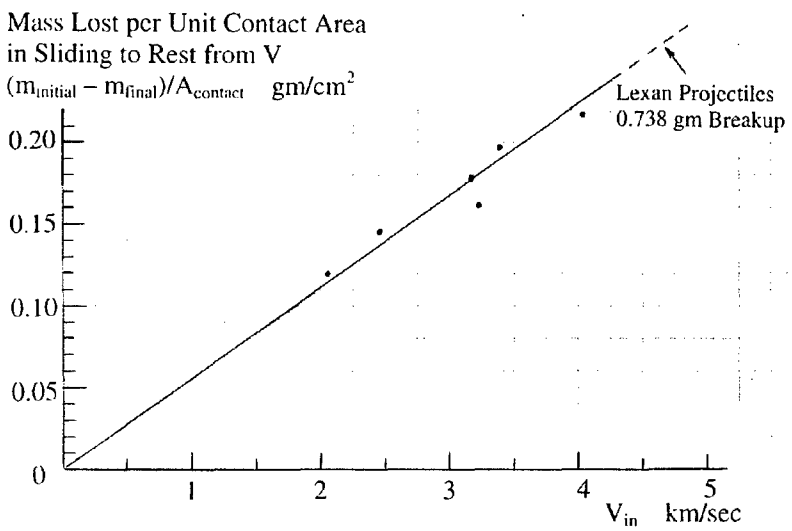

FIGURE 8. Mass Loss Data for 0.738 gram Lexan Projectiles that Slide to Rest in a Multi-Turn Soft Catch . For V_{in} = 3.5 km/sec about 50% of the 0.738 gram Projectile had Ablated Away, and above 4 km/sec the Projectiles Broke Up so data could not be obtained. For a Slingatron accelerating Identical Projectiles with a Net Force α times the Frictional Drag, one expects < α^{-1} times the above loss.

the projectile nose, and <> represents an average value of the argument integrated around the semicircle. The left side of equation 6 is the quantity plotted in Figure 7, and it is only equal to the friction coefficient in the limit that there is zero ablated mass from the projectile and also zero snowplowed dusty gas accumulated on the projectile nose. Figure 8 shows the mass loss of projectiles that were recovered from the soft catch .

Measurement of the asperity heights and microscopic examination showed that after repeated traversals by lexan projectiles up to ~ 5 km/sec, the track had become slightly smoother and harder, but use of a single 2.4 km/sec Al projectile resulted in shallow gouges [11].

POTENTIAL DEFENSE APPLICATIONS

Although the slingatron concept is in the design and computer-modeling phase, we note that it would have several advantages if it works as theorized. First, it is a simple mechanical device that does not involve a flow of high temperature high-pressure gas in the guide tube. The result (from the thermal calculations below) is that it appears capable of launching large mass projectiles at high velocity and high fire rates without overheating the guide tube, and without muzzle blast or EMP except from the drive motor.

Second, the accelerating coriolis force continues to provide projectile acceleration at high speeds, provided the sliding friction coefficient continues to decrease at least as 1/V with increasing velocity. This force is experienced along the length of an elongated projectile, and not just on its base. Third, the slingatron could be powered by a standard technology motor (internal combustion, turbine, or electrical) that continuously provides

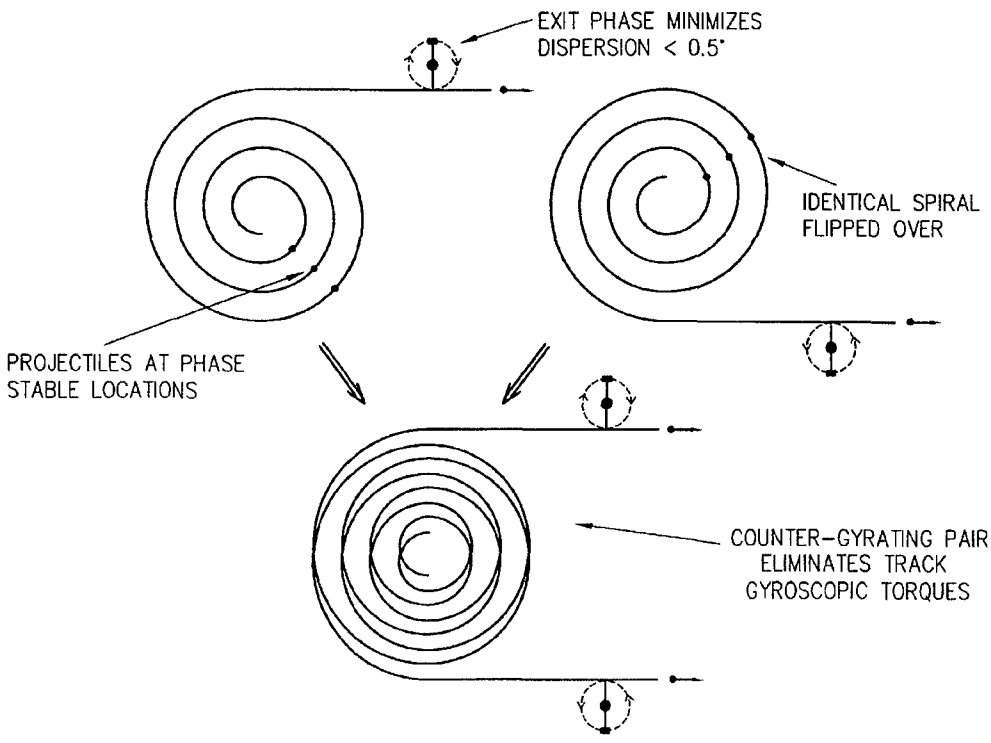

FIGURE 9. Two Counter-Gyrating Spirals that can be Re-Directed as a Unit without Precession-Inducing Torques. The Linear Exit Sections are chosen to have a length so that the Phase-Locked Projectiles Exit when the Swing Velocity is Parallel to the Tube, to Minimize Angular Dispersion at Launch.

energy to the spiral, which in turn directly couples its inertial energy into projectiles passing through the spiral. Finally, the device appears capable of accelerating a continuing stream of smart projectiles through the spiral with the maximum rate being limited by either the gyration frequency or the available power.

Figure 9 shows an arrangement in which 2 counter-gyrating spirals are assembled so that as a unit they can be swiveled for aiming without causing precession-inducing torques, and Figure 10 shows a concept of a rapid-fire slingatron based on this arrangement in which a turbine is shown powering the system.

The counter-gyrating spirals shown in Fig 9 are mounted on opposite sides of a common drive-plate structure, and the drive-plate would undergo a small-amplitude *linear* oscillation in response to the pair of counter-gyrating spirals. Ratchets could ensure that the spirals turn in opposite directions, and the drive plate ensures their locked frequency. Thus the pair of counter-gyrating spirals could be brought up to speed by a single high-powered motor that drives a small-amplitude linear oscillation of the drive plate. (This differs from the circular motion of the drive plate discussed in the context of a design for an experimental test in Figs 4 and 5.)

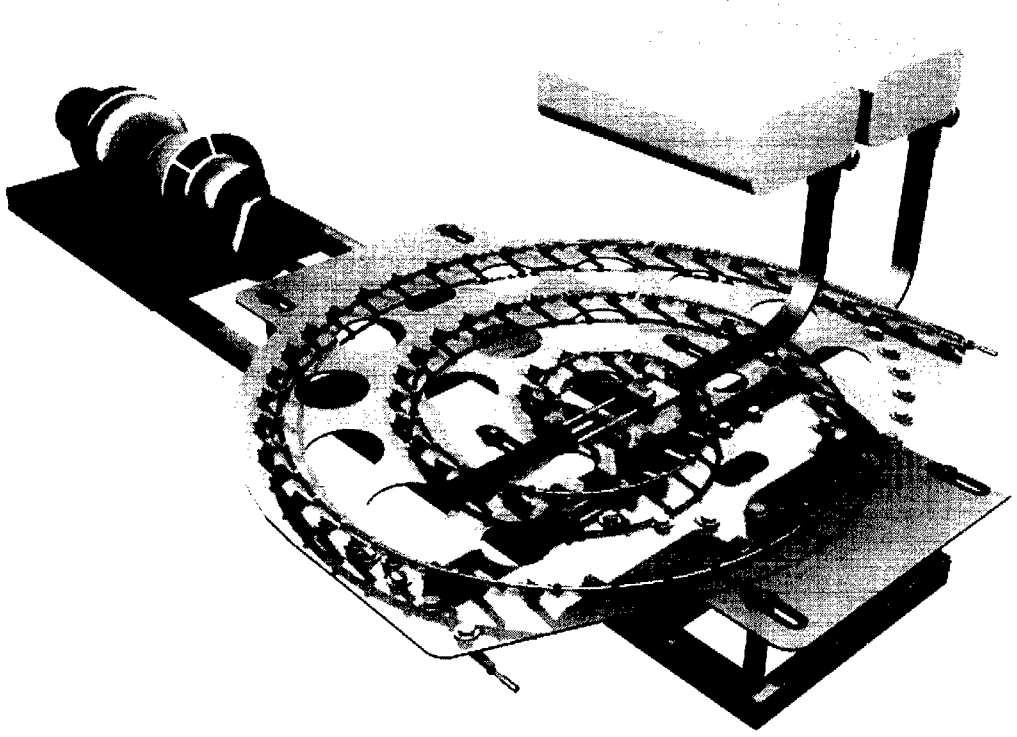

FIGURE 10. Concept for a Continuous-Fire Dual-Spiral Slingatron powered by a Turbine that Drives a Small-Amplitude Linear Oscillation of a Single Drive Plate. The Counter-Gyrating Spirals are located on opposite sides of the Drive Plate. It consumes kerosene and air and fires projectiles without cartridges.

Projectile Feed System

An example is shown in Fig 11. It consists of a loading block that is propelled by an electrically controlled piston along 2 rods on which it executes a linear oscillation with its maximum speed equal to the gyration speed v. The fire rate could thus be controlled, with a maximum of 0.5f to reduce stresses. The loading block picks up a projectile from a feed chute when the block reaches its maximum amplitude and has zero speed. The loading block then pushes the projectile (past a retaining stop) into the spiral entrance when the block and the spiral are moving adjacent and parallel with velocity v.

Example 1: 1kg Smart Projectiles Launched at 3 km/sec from a 40mm Tube.

Here we consider the case in which the prime power supply has sufficient power to provide a continuous fire rate that might suffice for some long-range missions. This enables one to directly power the spiral with a single prime power supply without any intermediate power-conditioning step, as shown in Fig 10.

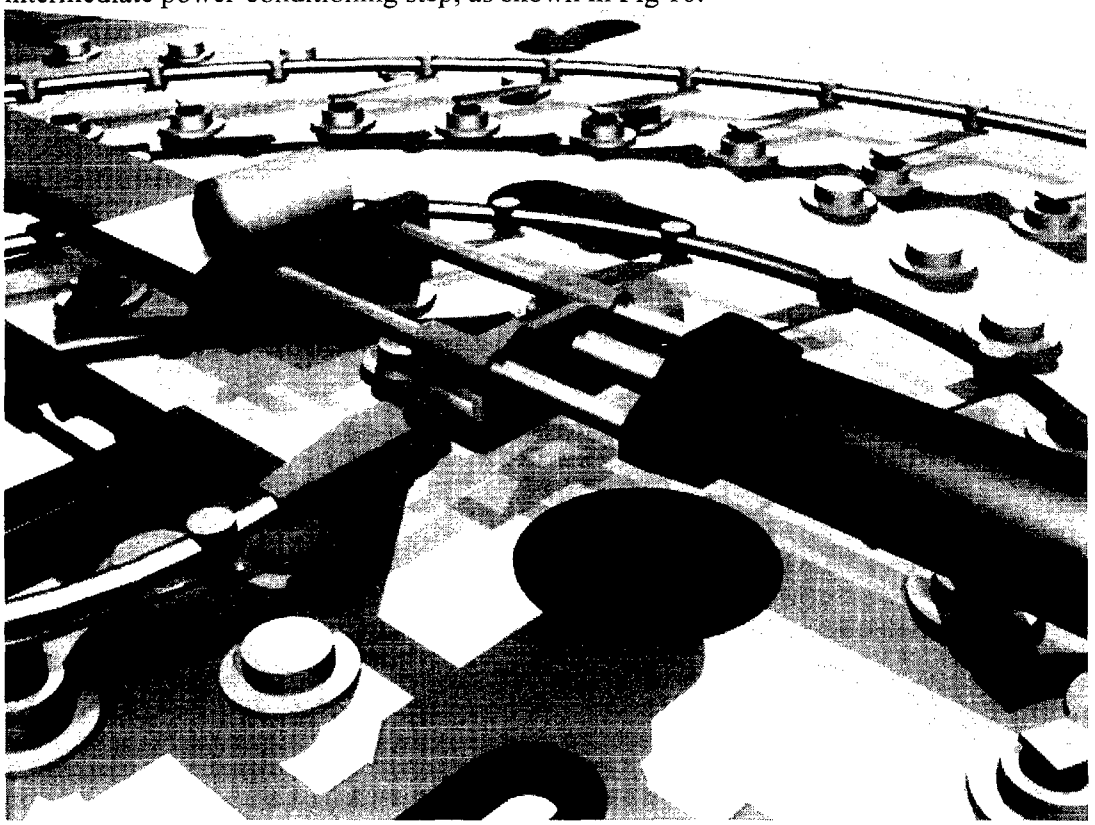

FIGURE 11. The loading block linearly oscillates along two rods. A projectile is transferred from a feed chute into the loading block when it is at its maximum amplitude, and subsequently pushed into the spiral entrance when the block and spiral entrance are moving parallel to each other with the same swing speed v.

For example, note that a single turbofan engine used on a 747 plane puts out 27.5 MW of power and weighs 4 tons. Assuming a turbine power unit with these numbers (without the bypass fan), and a launch efficiency of 50%, the slingatron could maintain a

continuous stream of smart 1 kg 3 km/sec projectiles with a fire rate of f_{shots} = 3 shots/sec, that might suffice for some ground-to-air-missions.

An example of a set of numbers for such a machine are: swing speed v = 200 m/sec, frequency f = 90 cps, tube ID = 4 cm and OD = 6 cm, swing radius r = 35.4 cm, final radius of curvature R = 5.31 meters, velocity gain per turn ΔV = 1.088 km/sec, number of turns in the spiral = 2.75, projectile diameter $d_p \sim 4$ cm, length l_p = 32 cm, and average mass density ρ_p = 2.5 gm/cc. Note, larger f gives a smaller R, e.g., f = 120 cps and V = 2.5 k/s gives R = 3.32 meters which would be suitable for a mobile platform.

Example 2: 50 kg Smart Projectiles Launched at 3 km/sec.

For this larger example, we note that 250MW turbines exist for example in some power generation plants. Assuming the same ~ 50% efficiency, a single turbine of this power could launch a steady stream of 50 kg projectiles at 3 km/sec with a continuous fire rate of 1 per 1.8 seconds.

Heating of a Spiral Slingatron Tube Used for a Continuous Stream of Shots

Although the slingatron delivers a relatively small thermal load into its guide tube, some heating does occur which we now estimate. In a continuous fire situation, repeated traversals of the track by projectiles will cause the track surface temperature to increase due to projectile sliding friction. Each projectile will impart a thermal pulse to the track and leave in its wake a temperature spike immediately behind the projectile. The track surface then cools as heat diffuses deeper into the tube wall until traversed by another projectile. This process continues and gradually increases the average temperature of the track. However, if this average heating occurs slowly enough, heat can diffuse through the guide tube wall and be removed from the outer surface by convection into the air through which it gyrates, in which case further temperature increase of the inner wall ceases. Here we derive some simple formulas for the spike and average temperature increases of the track and the potential for heat removal for continuous operation of the launcher. The projectiles are assumed to be simple cylinders of length l_p and diameter d comparable to the inner diameter of the guide tube.

The friction power dissipated by a single projectile is $\mu mV^3/R$ where R is the local radius of curvature of the guide tube. This power is shared by evaporation and heating of bearing gas from the projectile contact surface, and heating of the track throughout the semi-circular contact arc $\pi d/2$ swept out by the projectile. The contact pressure and friction power density are assumed constant throughout the half-cylinder contact surface of the projectile, and a fraction F of this friction power goes into track surface heating.

During a stream of shots the swept track experiences thermal flux pulses of duration l_p/V and power per unit area q, with a frequency f_{shots}, where $A = \pi d l_p/2$ is the projectile contact area. The power density q in a thermal pulse, and the average power <q> per unit area into the track area swept by repeated traversal pulses, are thus

$$q = \mu F m V^3/(AR) = \pi\mu F \rho_p d f V^2 ,$$
$$<q> = \mu(mV^2/R)(2Ff_{shots}/\pi d) = \pi\mu F \rho_p l_p d f f_{shots} V . \quad (7)$$

For the case of a constant heat flux q entering the surface of an infinitely thick slab of material (in this case steel), the heat diffusion equation has a simple solution for the increase in surface temperature $T_s(t)$ over its initial value T_o, namely

$$\Delta T(\text{degrees K}) = T_s(t) - T_o = 2qt^{1/2}(\pi\rho_s c_s \kappa_s)^{-1/2} = 0.84q(\text{watts/cm}^2)t_{scc}^{1/2}, \quad (8)$$

where for steel the parameters are, specific heat $c_s = 0.460$ Joules/(gmK), density $\rho_s = 7.83$ gm/cm^3, and thermal conductivity $\kappa_s = 0.502$ watts/(cmK). Combining (7) with (8) gives the temperature spike increase immediately behind a projectile, and the average increase in the track temperature of the track after many traversals, namely

$$\Delta T(\text{spike}) = 0.84q(l_p/V)^{1/2} = 8.34\mu F\rho_p fd(l_p V^3_{km/sec})^{1/2},$$
$$<\Delta T> = 0.84<q>t^{1/2} = 0.0264\mu F\rho_p d l_p f f_{shots} V_{km/sec} t^{1/2}, \quad (9)$$

where temperature rises are in degrees K, q in watts/cm^2, and in the final expressions on the right of (9) lengths, mass densities, frequencies, and times are in cgs units except for the velocities that are in km/sec as indicated. Note that f is constant throughout the spiral, so that $\Delta T(\text{spike})$ is proportional to $\mu V^{3/2}$ and $<\Delta T>$ to μV. If μ decreases with increasing V, then these increases in track temperature become less dependant on V.

Consider example 1 given in the preceding section, namely 1 kg projectiles launched at 3 km/sec at 3 per second, i.e., $f_{shots} = 3$ and use the slingatron numbers given in example 1. We will also assume that the sliding friction coefficient μ of such large projectiles at V = 3 km/sec is 0.005 and that the fraction of dissipated friction energy going into the guide tube is F = 0.2. For this choice using equation 9 we find $\Delta T(\text{spike}) = 221$ K, and $<\Delta T> = 6.84t^{1/2}$ for which the average temperature would go up by ~ 216K after 1000 seconds i.e., after 3000 shots. Such a slow average heating would have time to diffuse through the tube wall for disposal so the machine could be operated continuously.

Finally, from the scaling section in Ref. 5, one can multiply all the linear dimensions of a given design by the same number and one has a larger machine that is geometrically similar and as viable mechanically as the smaller machine from which one scaled. However, the temperature increase formulas (9) scale differently. Specifically, as m increases as α^3, the spike temperature increase ΔT behind the projectile increases as α (note $f \sim \alpha^{-1}$), and $<T>$ stays the same independent of α provided the shot rate f_{shots} is chosen to be proportional to f. Thus very large projectiles could also be launched with low thermal energy transfer to the guide tube wall, depending on experimental data for the friction coefficient μ and the fraction F of friction power transferred to track heating.

SUMMARY

The dynamics, mechanics, friction, and thermal physics of the spiral slingatron mass accelerator concept have been discussed, and projectile streams of high velocity appear possible and potentially useful for a variety of industrial, space, and energy

applications. Long tapered swing arms provide high swing speeds with lower gyration frequencies and may provide a path to extremely high projectile speeds.

If smart projectiles could be manufactured that were cheap and effective, and the slingatron works as theorized, such systems might also have a useful defense role. Projectiles would not have to individually strike a distant target, but need to be only smart enough to narrow down the rapid-fire stream and perhaps fragment on final approach.

ACKNOWLEDGMENTS

This work was supported by the Advanced Launch Corporation, including the sliding friction experiment up to 2 km/sec using a powder gun. The extension of the friction experiment into the velocity range above 2 km/sec using a light gas gun was supported by NASA via U.S. Army Contract/Order No. DAAD17-00-P-0710 with UTRON Inc. The author also wishes to thank Mr. Paul Westmeyer of the NASA-GSFC, many scientists at the U.S. Army Research Laboratory and UTRON Inc., Mr. Mark Kregel, and Dr Jonathan Jones of NASA-MSFC, for useful discussions.

REFERENCES

1. D. A. Tidman, Sling Launch of a Mass Using Superconducting Levitation, *IEEE Transactions on Magnetics*, Vol. 32, No. 1, January, 1996, pp 240-247 (accepted Dec. 28, 1994).
2. D. A. Tidman, Slingatron Mass Launchers, *Journal of Propulsion and Power,* Vol.14, No. 4, pp 537-544, July- August, 1998.
3. D. A. Tidman and J. R. Greig, Slingatron Engineering and Early Experiments, *Proceedings of the 14th SSI/Princeton Conference on Space Manufacturing*, May 6-9, 1999, ed. by B. Faughnan, publ. by Space Studies Institute, Princeton, NJ, pp 306-312.
4. D. A. Tidman, Method and Apparatus for Moving a Mass in a Spiral Track, *US Patent No. 6,014,964*, January 18, 2000.
5. D. A. Tidman, The Spiral Slingatron Mass Launcher, *Proceedings of the Space Technology and Applications International Forum,* February 11, 2001, publ. by the American Institute of Physics.
6. G. R. Cooper, D. A. Tidman, and M. Bundy, Numerical Simulations of the Slingatron, *submitted to the 10th U.S. Army Gun Dynamics Symposium*, April 23-26, 2001, Austin, Texas.
7. M. Bundy, G. R. Cooper, and S. Wilkerson, Optimizing a Slingatron-Based Space Launcher Using Matlab, *submitted to the 10th U. S. Army Gun Dynamics Symposium*, April 23-26, 2001, Austin, Texas.
8. Cyril M. Harris, Shock and Vibration Handbook, *publ. by McGraw Hill, Fourth Edition,* 1996.
9. B. D. Tapley, Eshbach's Handbook of Engineering Fundamentals , *publ. by John Wiley & Sons, Fourth Edition,* 1990.
10. D. A. Tidman, A Scientific Study on Sliding Friction Related to Slingatrons, *ALC Tech Note 2001-1*, Final Report for U.S. Army Contract No. DAAD17-00-P-0710, 2/20/01.
11. F. Stefani and J. V. Parker, Experiments to Measure Gouging Threshold Velocity for Various Metals Against Copper, *IEEE Trans. Magnetics,* Vol. 35, Jan 1999, pp. 312-316.